Polymer Vol. 39 No. 23, pp. 5609–5617, 1998
0032-3861/98/$ – see front matter

PII: S0032-3861(98)00015-9

TMXDI-based poly(ether urethane)/polystyrene interpenetrating polymer networks: 2. T_g behaviour, mechanical properties and modulus-composition studies

Douglas J. Hourston[a,*], Franz-Ulrich Schäfer†[a], Michael H.S. Gradwell[a] and Mo Song[b]

[a]*Institute of Polymer Technology and Materials Engineering, Loughborough University, Loughborough, Leicestershire LE11 3TU, UK*
[b]*School of Physics and Chemistry, Lancaster University, Lancaster LA1 4YA, UK*
(Received 15 November 1996; revised 30 October 1997; accepted 5 December 1997)

In this, the second of two papers on a series of simultaneous polyurethane (PUR)/polystyrene (PS) interpenetrating polymer networks (IPNs), the T_g behaviour, mechanical properties and modulus–composition relations have been studied. A gross phase morphology over the full IPN composition range was indicated by two separate loss factor peaks from dynamic mechanical thermal analysis (DMTA). Both DMTA and modulated-temperature differential scanning calorimetry (MT-d.s.c.) measurements revealed that the T_g of the PS transition increased with decreasing PS content in the IPN. This was explained by an increase in interactions between the PUR hard segments and the π-electrons of the PS phenyl rings. Despite the phase-separated morphology, materials with good mechanical properties were obtained. The tensile properties and the Shore hardness results were comparable to similar semi-miscible PUR/PEMA IPNs. The Budiansky modulus–composition relation resulted in the best fit with the experimental data, indicating phase inversion at mid-range compositions. Modulus–composition studies, indicating that phase inversion occurred at the 30:70 PUR/PS IPN composition, corroborated the electron microscopy findings from the first paper in this series.

(Keywords: interpenetrating polymer networks; glass transition behaviour; modulus-composition studies)

INTRODUCTION

Polyurethane (PUR)/polystyrene (PS) interpenetrating polymer networks (IPNs) have been the subject of a considerable amount of research[1]. Yet, despite this level of interest, few detailed studies[2,3] have been conducted to investigate the changes in morphology and properties over the full PUR/PS IPN composition range. In this study, the entire composition range was studied using 10% weight increments. While most research on PUR/PS IPNs has been conducted using diphenylmethane diisocyanate or toluene diisocyanate in the PUR hard segment, in this study a tertiary aliphatic tetramethylxylene diisocyanate (TMXDI) was used. In the first paper[1] of this series, the reaction kinetics, investigated using FT-i.r., and the morphology, as observed by scanning (SEM) and transmission (TEM) electron microscopy, were discussed. In addition, the thermal properties were studied by thermogravimetric analysis.

The aims of this study were to investigate the behaviour of the glass transition temperature (T_g) and the mechanical properties of the full PUR/PS IPN composition series. The composition where phase inversion occurred was determined using modulus composition models, and the IPN morphology, as seen from electron microscopy[1], was related to the dynamic mechanical and mechanical properties. Furthermore, this immiscible PUR/PS IPN composition series was compared to a semi-miscible PUR/PEMA composition series[4]. The characterization techniques employed included dynamic mechanical thermal analysis, modulated-temperature differential scanning calorimetry, stress–strain and hardness measurements.

* To whom correspondence should be addressed
† Present address: BASF AG, D-67056 Ludwigshafen, Germany

EXPERIMENTAL

Materials and IPN preparation

The materials and syntheses of the IPNs were given in the first paper[1] and in an earlier publication[5]. In brief, the crosslinker trimethylol propane (TMP, Aldrich) was dissolved in the poly(oxypropylene) glycol of 1025 molar mass (PPG1025, BDH) at 60°C. Azo-isobutyronitrile (AIBN, BDH) was dissolved in a mixture of styrene (S, Aldrich) and divinylbenzene (DVB, Aldrich) and subsequently added to the first mixture. After the addition of the stannous octoate (SnOc, Aldrich) and the 1,1,3,3-tetramethylxylene diisocyanate (TMXDI, kindly donated by Cytec), the components were stirred under nitrogen for 5 min. After degassing for 1 min at high vacuum, the mixture was cast in stainless steel spring-loaded O-ring moulds, which had been pre-treated with CIL Release 1711 E release agent. The curing cycle consisted of three stages: 24 h at 60°C, 24 h at 80°C and 24 h at 90°C.

IPN characterization

Dynamic mechanical thermal analysis (DMTA) measurements were performed with a Polymer Laboratories MK II Dynamic Mechanical Thermal Analyzer. The samples were measured in the bending mode (single cantilever) at a fixed

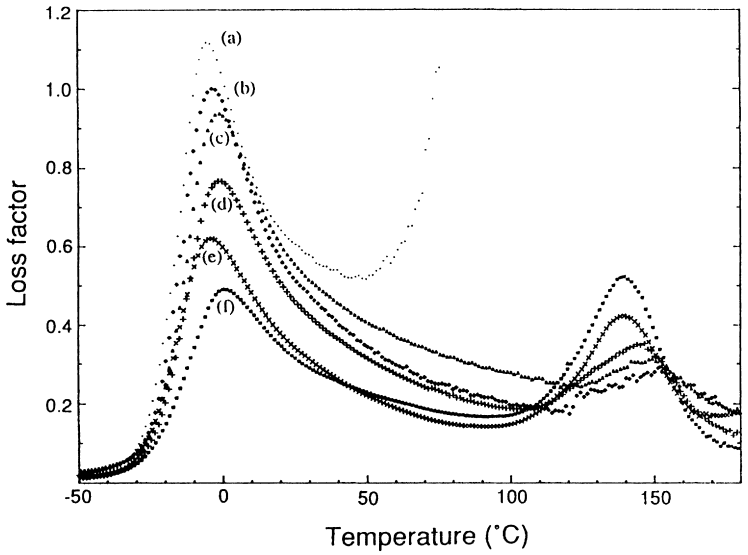

Figure 1 Loss factor (tan δ) *versus* temperature data for PUR/PS IPN compositions. (a) Pure PUR; (b) 90:10, (c) 80:20, (d) 70:30, (e) 60:40 and (f) 50:50 PUR/PS

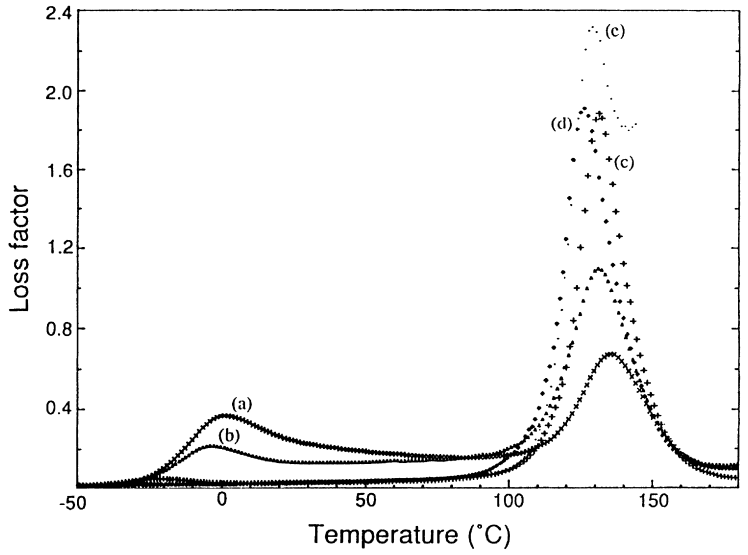

Figure 2 Loss factor (tan δ) *versus* temperature data for PUR/PS IPN compositions. (a) 40:60 PUR/PS; (b) 30:70, (c) 20:80, (d) 10:90 and (e) PS

frequency of 10 Hz from −60 to 200°C using a heating ramp of 3°C/min. The 3 mm thick test specimens were cut to a rectangular shape with 50 × 10 mm dimensions. The applied strain setting was ×4.

Modulated-temperature differential scanning calorimetry (MT-d.s.c.)[6] is a new extension of conventional d.s.c.. Among the advantages of MT-d.s.c. over conventional d.s.c. are enhanced sensitivity and improved resolution[7]. Applying a sinusoidally varying heating programme to the polymer sample makes it possible to distinguish between reversible and irreversible phenomena and disentangle overlapping events. The glass transition temperatures were determined using a TA Instruments DSC 2910 Analyzer fitted with a MDSC™ module. Measurements under nitrogen were conducted from −70 to 150°C at a heating rate of 3°C/min. The oscillation amplitude was ±1.5°C and the period 60 s.

Stress–strain analyses were conducted using a J.J. Lloyd 1 2000R Tensometer equipped with a 500 N load cell and a crosshead speed of 50 mm/min. Small dumb-bells with a gauge length of 30 mm were used in this study. Tests were conducted at 23 ± 1°C and the values quoted are an average of four or five samples.

Shore A hardness was determined using a Zwick model 3114 instrument, whilst Shore hardness D was measured using a Jamaica Instruments gauge. The testing was conducted at room temperature (23 ± 1°C). Hardness values quoted are an average of eight readings taken at random over the entire specimen surface.

RESULTS AND DISCUSSION

Dynamic mechanical thermal analysis

The morphology and miscibility of two polymer components greatly influences[8,9] the mechanical properties of a polymer blend and can be assessed[10] from DMTA data. Two separate loss factor peaks indicate[11] an immiscible system, whereas one peak indicates a high degree of miscibility, although the latter only applies to polymers with T_g values that are more than 10–20°C apart. An intermediate degree of miscibility results in a broad almost rectangular transition. This microheterogeneous

Table 1 DMTA (10 Hz) and MT-d.s.c. data for the PUR/PS IPNs and the homonetworks as a function of composition

Composition PUR/PS IPN (% PS)	DMTA					MT-d.s.c., T_g (°C)	
	T_g (tan δ, °C)		tan $\delta_{maximum}$		Inter-transition height at 67°C	PUR	PS
	PUR	PS	PUR	PS			
0	−5	—	1.10	—	—	−34	—
10	−4	150	1.00	0.28	0.24	−34	—
20	−2	148	0.94	0.31	0.32	−34	113
30	−1	146	0.77	0.35	0.22	−36	112
40	−3	140	0.62	0.42	0.17	−36	113
50	1	139	0.49	0.52	0.18	−37	114
60	2	136	0.37	0.67	0.16	−36	113
70	−4	131	0.21	1.11	0.13	−37	110
80	−20	131	0.10	1.82	0.03	−38	108
90	−22	127	0.02	1.91	0.03	—	100
100	—	128	—	2.30	0.02	—	100

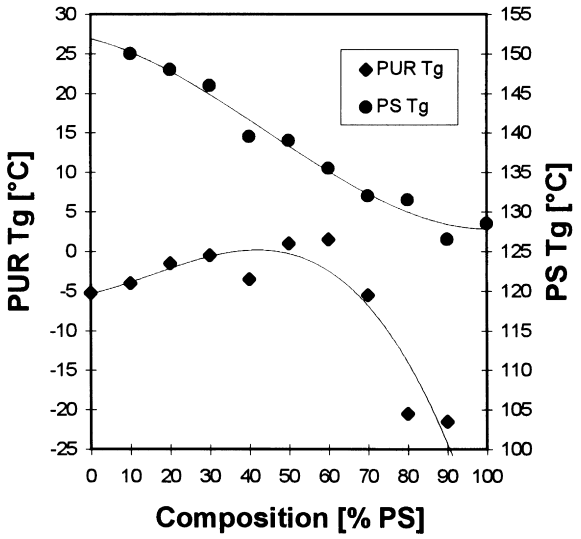

Figure 3 Component T_g location (tan δ, 10 Hz) *versus* composition

morphology is often used to develop good damping materials[4]. The parameters of interest in this study were the respective loss factor peak heights, the values for the loss factor at the inter-transition region and the loss factor peak locations (to assess the IPN miscibility and phase continuity). The loss factor *versus* temperature data for the PUR/PS IPN composition series crosslinked with a PPG1025/TMP ratio of 3:1 and 5 mol.% DVB are shown in *Figures 1* and *2*. The DMTA data are given in *Table 1*. As expected for an immiscible polymer pair, two well-separated loss factor transitions were observed, with low values in the inter-transition region. Compared to the two homopolymer networks, a shift of the loss factor location, i.e. of the glass transition temperatures, took place in the composition series. *Figure 3* shows the T_g values *versus* IPN composition of the materials, as obtained from the peak of the loss factor (10 Hz). Comparing the IPNs to the homopolymer networks, a T_g shift with changing composition was observed for both polymers. The PUR transition shifted to slightly higher temperatures, from −5 to 2°C, as the PUR weight fraction decreased from 100:0 to 40:60 PUR/PS (*Table 1*). From the 30:70 PUR/PS composition on, it fell considerably to a T_g of −22°C for the PUR in the 10:90 PUR/PS composition. The PS transition consistently shifted to lower temperatures with increasing PS weight fraction. The decrease was significant, with a difference of more than 20°C between the PS transition in the 90:10 PUR/PS IPN (150°C) and the PS homonetwork (128°C). Similar results showing higher T_g values for the PS transition have been observed in other PUR/PS IPN composition series with lower crosslink densities[12], with an isophorone diisocyanate (IPDI)-based PUR/PS IPN[13] and with a linear diphenylmethane diisocyanate-based PUR/linear PS mechanical blend[14]. The increase in the PS transition at higher PUR contents indicated that PS segments were less free to move in the IPNs than in the pure PS network. Reasons for this could be an increase in crosslink density through grafting or some other specific intermolecular interactions[15] between the PS and PUR polymer chains. A PS T_g shift to higher temperatures has also been observed in high-impact polystyrene[16]. It was proposed[16] that the area of contact between the PS and the polybutadiene influenced the PS T_g. An increase in crosslink density of the matrix because of grafting also shifted the PS T_g to higher temperatures[16]. In a study on mechanical blends of linear PUR and PS, Theocaris and Kefalas[14] proposed that interactions of the π-electrons of the aromatic ring-containing PUR hard segments, with the PS phenyl side groups, were responsible for the increase in PS T_g in the polymer blends. The rigid hard segments were believed[14] to have had a T_g in the order of 160°C. Chugthai[13] suggested that some kind of anti-plasticization effect and essentially pure PS phases were the causes of the PS T_g shift in IPDI-based PUR/PS IPNs. However, none of these explanations were directly applicable to the PUR/PS IPNs of this study. No unsaturation was present in the PUR component of the PUR/PS IPN and the syntheses were conducted under comparatively mild conditions, so that no significant grafting would have occurred. Cowie[15] pointed out that not only interactions between π-electrons of phenyl rings have been observed, but that the π-electrons of a phenyl ring can interact with lone pair electrons, as observed[17] in PS/polyvinylmethylether blends. In the present study, interaction of the PS π-electrons with the lone pair electrons of the ether oxygen in the PUR soft segment or the lone pair electrons of the nitrogen atoms in the hard segments would have been possible. However, because of the much higher ether oxygen content compared to nitrogen, a PS T_g shift to

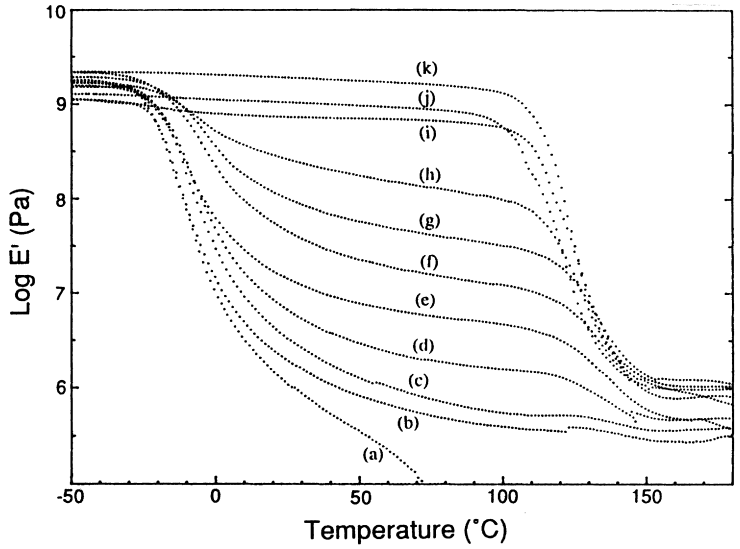

Figure 4 Log storage moduli *versus* temperature. (a) PUR; (b) 90:10, (c) 80:20, (d) 70:30, (e) 60:40, (f) 50:50, (g) 40:60, (h) 30:70, (i) 20:80, and (j) 10:90 PUR/PS; and (k) PS

lower temperatures and increased phase mixing with the PUR soft segment would have been expected. The opposite effect was, however, observed in this study.

A recent FT-i.r. study[18] on hydrogen bonding of linear PURs in a styrene solvent has shed new light on this phenomenon. Feve and co-workers[18] found that when increasing the amount of styrene solvent from 0 to 90% in the solution, an additional N–H stretching vibration appeared. This absorption peak was found between the free and the carbonyl group hydrogen-bonded N–H stretching at 3447 and 3347 cm^{-1}, respectively. In their opinion, the additional vibrational band that appeared at 3400 cm^{-1} was due to the hydrogen-bonded N–H stretching between the N–H and the π orbitals of the aromatic rings of the PS. The fact that this band was located between the free and the hydrogen-bonded N–H stretching gave an indication of its average strength. Thus, interaction of the N–H hydrogen of the rigid PUR hard segment with π orbitals of the PS phenyl rings could have led to an increase in PS T_g. This effect was more pronounced at higher PUR compositions in the PUR/PS IPN since more urethane links were present. More importantly, the PS domain sizes decreased considerably from 200 nm to 2 μm for the 50:50 PUR/PS IPN composition to 50–100 nm for the 90:10 composition[1]. This PS domain size decrease resulted in a greater surface area and, hence, a larger higher contact area with the PUR. This explained why the PS T_g of the 90:10 PUR/PS IPN was the highest at 150°C compared to 128°C for the PS homonetwork (*Table 1*). The much less significant increase of T_g for the PUR component from pure PUR to the 40:60 PUR/PS composition might be explained by increased phase mixing with the PS. A decrease of the PUR transition was observed from the 30:70 to the 10:90 composition. A similar phenomenon has been attributed to plasticization effects in polymer blends[19,20]. Dissolved PS chains in PUR domains might have disrupted the interactions between urethane links. More likely in this study, however, is that the PUR network was incompletely formed[4,19]. Consequences of an incomplete reaction are more dramatic[21] in step-growth polymerizations than in radically polymerized materials because of a much steeper fall in molar mass at lower conversions. Thus, a lower molar mass PUR polymer/oligomer would lead to a T_g shift towards lower temperatures.

The trend of the loss factor peak height of the components clearly followed composition (*Table 1*). At these cross-linking levels, the PS loss factor values were generally higher than those of the PUR of equal content in the IPN. The PUR loss factor decreased almost linearly with decreasing PUR content from 1.10 for the pure PUR to 0.02 for the 10:90 PUR/PS IPN. For the PS loss factor values a different trend was observed. A slow increase up to the 40:60 PUR/PS composition ($\tan\delta = 0.67$) was followed by a higher loss factor (1.10) for the 30:70 and very high values of 1.80 and 1.90 for the 20:80 and 10:90 IPNs, respectively. The loss factor peak height usually gives an indication of phase continuity in a polymer blend, the material exhibiting the higher peak representing the more continuous phase, whereas two transition peaks of the same height may be an indication of dual phase continuity[22]. From the data in *Table 1*, it can be concluded that phase inversion took place between the 60:40 and the 50:50 PUR/PS IPN compositions. However, it could also be argued that, due to the large differences in loss factor of the pure polymers, 1.10 for PUR and 2.30 for PS, that the equal peak height criteria may be misleading. The sharp increase in loss factor at the 30:70 composition points to a phase inversion at a higher PS content. The loss factor values of the inter-transition region (*Table 1*) were taken at an intermediate temperature (67°C) between the PUR and PS homonetwork glass transitions. Generally, the inter-transition loss factor values were very low and decreased with decreasing PUR content in the IPN. The low values were an indication of very limited phase mixing and little interface area in the IPNs.

The storage moduli *versus* temperature plots for the PUR/PS IPN composition series are shown in *Figure 4*. The storage moduli reflected the trend of the loss factor values. A pronounced drop in modulus occurred at the PUR and PS transitions. The two-step drop mechanism of the storage moduli indicated[9,22] gross phase separation in the IPNs. With increasing volume fraction of PS, the rubbery plateau between the PUR T_g and the PS T_g increased to higher moduli reflecting the change in composition. The 20:80 PUR/PS IPN exhibited a high modulus plateau between the PUR and the PS transition. A similar finding had been made with the comparatively high loss factor peak height

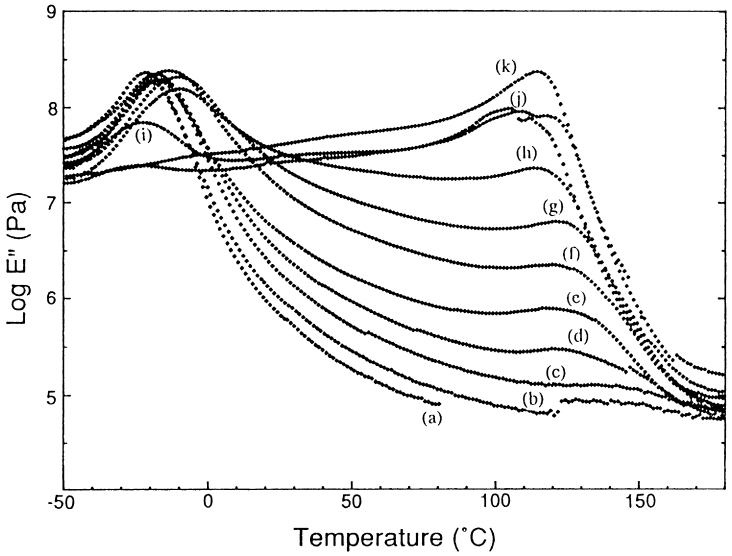

Figure 5 Log loss moduli *versus* temperature for the PUR/PS compositions. (a) PUR; (b) 90:10, (c) 80:20, (d) 70:30, (e) 60:40, (f) 50:50, (g) 40:60, (h) 30:70, (i) 20:80, (j) 10:90 PUR/PS; and (k) PS

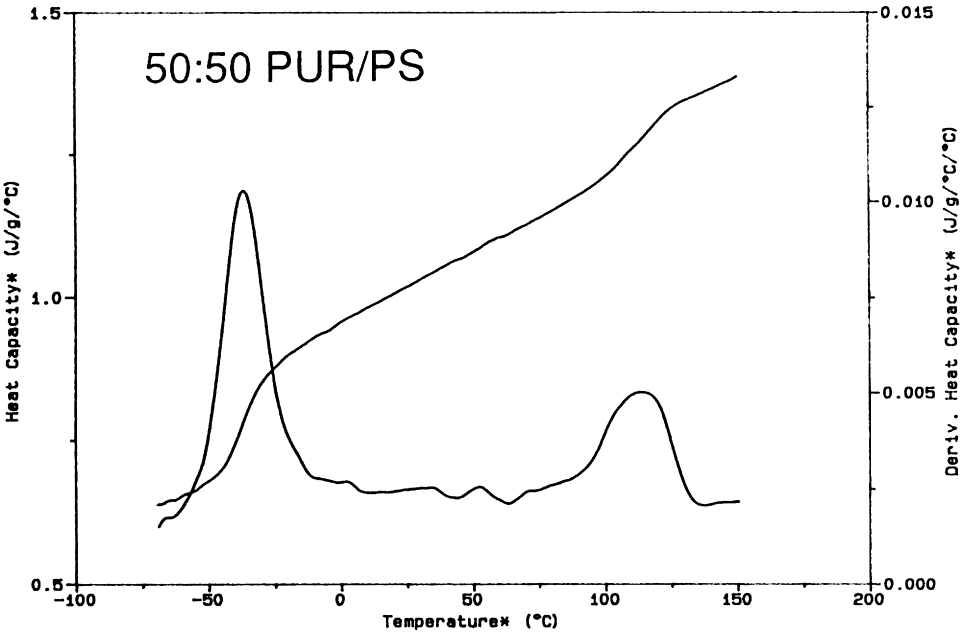

Figure 6 MT-d.s.c. trace of the 50:50 PUR/PS IPN composition

Table 2 Mechanical properties of the PUR/PS IPN as a function of composition

Composition PUR/PS IPN(% PS)	Tensile properties				Hardness, Shore	
	Stress at break (MPa)	Strain at break (%)	Young's modulus (MPa)	Toughness (J)	A	D
0	1.2	210	1.0	0.6	40	25
10	2.4	430	1.1	2.0	43	25
20	4.2	530	1.7	4.0	49	27
30	12	770	4.3	14	59	35
40	13	310	7.2	4.2	75	41
50	10	230	10	2.3	83	52
60	7	83	33	0.6	94	59
70	14	20	83	0.3	96	68
80	36	8	830	0.4	98	95
90	45	7	1000	0.5	99	96
100	47	7	1300	0.4	99	97

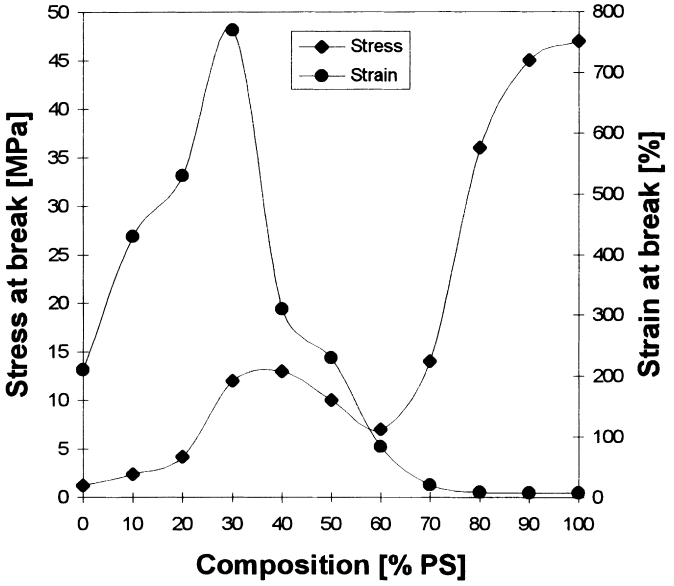

Figure 7 Stress and strain at break *versus* PUR/PS IPN composition

(*Figure 2*) indicating a change in the IPN morphology, i.e. continuous phase.

The loss moduli *versus* temperature showed two distinct transitions (*Figure 5*). Similar to the results from the loss factor data, the PUR exhibited its highest T_g in the 40:60 PUR/PS sample. The PS transition decreased with decreasing PS content. The PUR loss modulus peak was predominant from the 90:10 to the 30:70 compositions. The change in the dominant peak occurred between the 30:70 and 20:80 PUR/PS composition, again indicating a change of IPN morphology.

Modulated-temperature d.s.c.

MT-d.s.c. measurements were conducted as a second technique to investigate the T_g behaviour of the PUR/PS IPNs. While conventional d.s.c. did not prove sensitive enough to detect both T_g values in the IPNs, the T_g values were detected over most of the IPN composition range using MT-d.s.c.[6,7]. The T_g values for the homonetworks, as taken from the peaks of the derivative of heat capacity *versus* temperature plots, were −34°C for the PUR and 100°C for the PS (*Table 1*). The higher transition values of −5 and 128°C obtained from the DMTA loss factor peaks (10 Hz), being due to the dynamic nature of the experiment. The PUR transition decreased slightly from −34°C for the PUR network to −38°C for the transition in the 20:80 PUR/PS IPN (*Table 1*). The PS transition obtained from MT-d.s.c. showed the T_g values shifting to lower temperatures with increasing PS content. The PS transition of the 80:20 PUR/PS IPN was at 113°C and, thus, 13°C higher than that of the PS homonetwork (100°C). The higher peak height of the PUR, as shown in the 50:50 PUR/PS IPN (*Figure 6*), was as a result of the greater change in heat capacity[22] of PUR compared to that of PS for the transition.

Mechanical properties

The mechanical properties of the composition series were investigated by tensile testing and Shore A and D hardness measurements. The stress and elongation at break, Young's modulus, the toughness index and values for Shore A and D hardness are given in *Table 2*. As expected, an important change in the mechanical properties was observed when combining an elastomer with a plastic. A plot of the stress and strain at break *versus* IPN composition is shown in *Figure 7*. Stress at break values were low (below 5 MPa) for the 90:10 and 80:20 PUR/PS IPNs, but they increased with increasing PS content to 13 MPa for the 60:40 PUR/PS IPN. After that, they fell again to a value of 7 MPa for the 40:60 composition before increasing dramatically, from the 30:70 composition onwards. This trend can be explained by looking at phase continuity of the IPNs, as the continuous phase is known[22] to have a large influence on the mechanical properties of IPNs. From the DMTA data, it was believed that phase inversion took place between the 60:40 and 20:80 PUR/PS IPN compositions. The increasing stress at break values up to the 60:40 IPN could be explained by the reinforcing effect of the PUR by the PS. Increasing the PS content further would lead to larger PS domains and, as a consequence, a decreased phase continuity of the PUR network. This weaker PUR network would lead to lower stress at break values. It was only at the 30:70 PUR/PS composition that the PS phases exhibited some degree of phase continuity, which could account for the increasing stress at break values. At the 20:80 PUR/PS IPN, PS was shown by SEM to be the continuous phase[1]. This manifested itself in a steep increase in stress at break from 14 MPa for the 30:70 to 36 MPa for the 20:80 PUR/PS IPN composition. These assumptions were in agreement with the previous findings[1] from TEM and SEM studies. The strain at break *versus* IPN composition exhibited a different trend (*Figure 7*). The strain at break values went through a maximum of 770% at the 70:30 PUR/PS IPN composition, but much lower values were recorded for IPNs with higher PUR contents and even lower values for IPNs with lower PUR contents. The increase in strain at break from pure PUR to the 70:30 PUR/PS IPN compositions could be explained by a decrease in the tightness of the PUR network because of the PS domains. The PUR chains were able to align and the resultant more loosely bound network only broke at higher elongations. The decrease in strain at break from the 60:40 PUR/PS IPN to the pure PS was the result of a combination of two factors. From the 60:40 to the 30:70 PUR/PS compositions, the PUR content decreased as did the

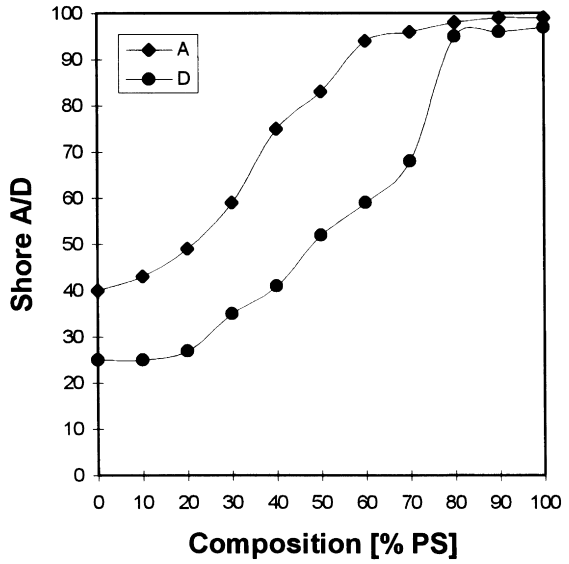

Figure 8 Shore A and D hardness *versus* PUR/PS IPN composition

extent of phase continuity of the PUR. The extremely low values for the strain at break for compositions where PS represented the continuous phase (from 20:80 to 10:90 PUR/PS) were as expected for PS at room temperature.

Because of the high strain at break value, the toughness index, a function of stress and strain, also exhibited a maximum at the 70:30 composition (*Table 2*). Young's modulus values followed a trend similar to the stress at break, increasing with increasing PS weight percent (*Table 2*). A sharp increase from 83 to 830 MPa took place between the 30:70 and 20:80 PUR/PS IPN compositions. A detailed description of the modulus–composition behaviour is given in a subsequent section.

Plots of Shore A and D values against IPN composition are shown in *Figure 8*. Shore A hardness values exhibited a sigmoidal curve shape. A slightly higher than expected increase in Shore A hardness occurred between the 70:30 and 60:40 PUR/PS compositions, possibly indicating a change in the continuous phase. The useful working ranges[23] for the Shore hardness measurements are between 10 and 90 for Shore A (between 30 and 90 for Shore D) and, therefore, reliable results for Shore A were only obtained for compositions up to a PS content of 50%. Shore D hardness values showed a linear increase with increasing the PS content from the 70:30 to the 30:70 PUR/PS composition. A significant increase in hardness was observed between the 30:70 (Shore D 68) and the 20:80 (Shore D 95) PUR/PS compositions. A behaviour similar to the Young's modulus was not surprising since hardness is directly related[9] to modulus and strength. Thus, from Shore A measurements, a slight increase in hardness at about the 70:30 PUR/PS composition was noted, whereas from Shore D, a large increase was observed between the 30:70 and 20:80 PUR/PS IPN compositions.

Modulus–composition models

The phase continuity and phase inversion in polymer blends can be studied by relating[9] the shear or tensile moduli to modulus–composition models. Several theories[24–27] have been reviewed by Nielsen[28,29], Dickie[30] and Hourston and Zia[31]. Kerner[27] derived a theory for a matrix with spherical inclusions. The upper and lower bounds of the modulus of this two-phase polymer material are given by equation (1).

$$\frac{G}{G_1} = \frac{(1-\phi_2)G_1 + (\alpha+\phi_2)G_2}{(1+\alpha\phi_2)G_1 + \alpha(1-\phi_2)G_2} \tag{1}$$

Here, subscripts 1 and 2 refer to the matrix and the inclusions, respectively. G is the shear modulus, ϕ is the volume fraction and α is a function of the matrix Poisson ratio, ν_1, $\alpha = 2(4-5\nu_1)/(7-5\nu_1)$. A model which predicts phase inversion at mid-range compositions in two-phase polymer systems was developed by Budiansky[26]. This model assumes that the dispersed phase becomes the continuous one at some point in the mid-composition range.

$$\frac{\phi_1}{1+\epsilon\left(\frac{G_1}{G}-1\right)} + \frac{\phi_2}{1-\epsilon\left(\frac{G_2}{G}\right)-1} = 1 \tag{2}$$

Again, ϕ is the volume fraction, $\epsilon = 2(4-5\nu)/15(1-\nu)$, ν is the Poisson's ratio of the composite, G is the shear modulus and subscripts 1 and 2 represent the component polymers. A general mixing equation which often successfully predicts certain properties of composites with two continuous phases has been presented by Nielsen[29].

$$P^n = \phi_1 P_1^n + \phi_2 P_2^n, \quad -1 < n < 1 \tag{3}$$

P is a property such as elastic modulus or thermal conductivity and n is a function of the morphology of the system. For $n = 1$, the ordinary rule of mixtures results, whereas $n = -1$ describes the inverse rule of mixtures. The logarithmic rule of mixtures[9] arises when $n = 0$. The Davies[24,25] equation, which Hourston and Zia[31] class as a special solution to the Nielsen[29] equation, is designed for systems in which both components are present as continuous phases. It is given by equation (4), where G and ϕ have been defined previously.

$$G^{1/5} = \phi_1 G_1^{1/5} + \phi_2 G_2^{1/5} \tag{4}$$

In general, conversion from the shear to the tensile modulus, E, can be done using the equation $E = 2G(1+\nu)$. However, this was not done since the error that is introduced by using E in the expressions for G is small[32]. Poisson's ratio for the homopolymers was assumed to be 0.5 for the PUR and 0.35 for the PS[33], and Poisson's ratio for the various compositions was calculated using the weighted average[32,33] of the Poisson's ratio of the two components.

To date, the fit of experimental data to modulus–composition theories has been contradictory[4]. A number of researchers[31,34,35] found the Davies equation to describe best their experimental data. Others[4,33,36] found a better fit with the Budiansky equation. Investigating simultaneous and sequential PUR/PMMA IPNs, Akay and Rollins[36] found the elastic modulus–composition plots to comply with Budiansky's phase inversion model for simultaneous IPNs, and a dual-phase continuity model (Davies equation) for sequential IPNs. The dynamic storage moduli, however, behaved according to the Davies equation. Two factors might account for the controversial results. In most of these studies, the conclusions drawn were based on three and four composition points[37], which makes it difficult to make predictions over the whole composition range. Furthermore, Hourston and Schäfer[4] found in a recent study that the composition of the apparent phase inversion in log E' *versus* composition plots was dependent upon the temperature at which the moduli were taken. It was noticed[4] that when the dynamic moduli were studied at a temperature close to the

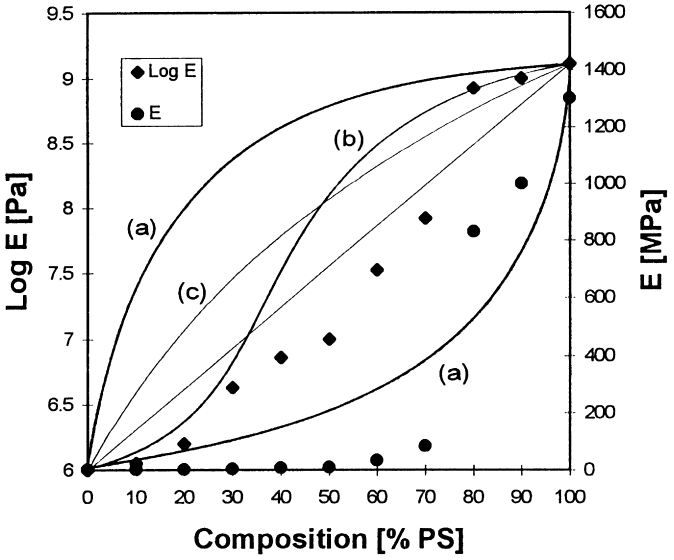

Figure 9 Log Young's modulus E and linear E *versus* composition and modulus–composition curves. (a) Kerner, (b) Budiansky and (c) Davies models

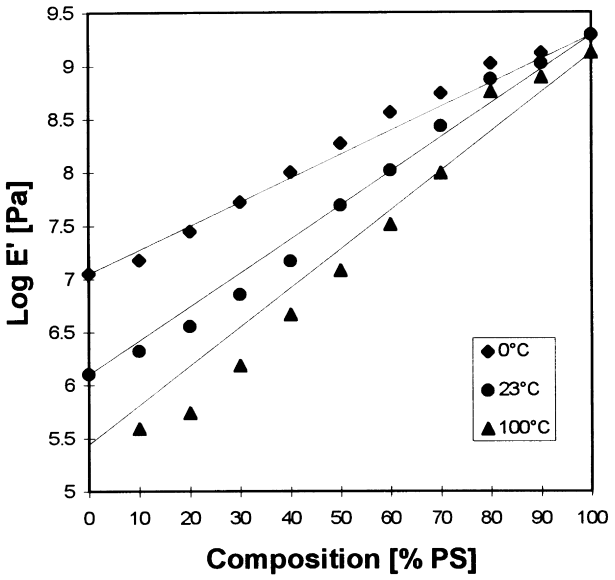

Figure 10 Log dynamic storage moduli *versus* IPN composition taken at 0, 23 and 100°C

T_g of the lower T_g component, a Davies-like behaviour resulted, whereas at the intermediate temperature, between the T_g values of both components, a Budiansky-like behaviour was observed.

Figure 9 shows the Young's moduli (obtained from tensile testing at room temperature) *versus* IPN composition together with four modulus–composition models. The experimental data showed some scatter and did not fit any of the models. However, some similarity with the Budiansky model which predicts phase inversion at mid-range compositions existed. The experimental data suggested that phase inversion took place between the 30:70 and the 20:80 PUR/PS IPN compositions. In addition to log E, a linear plot of E *versus* composition is shown to illustrate the pronounced increase in E between the 30:70 and the 20:80 composition. In addition to the Young's moduli, the dynamic (10 Hz) storage moduli E' of the IPNs and homonetworks were plotted against the composition in *Figure 10*. The storage moduli were taken at three different temperatures (0, 23 and 100°C). Again, the experimental data points for the storage moduli did not fit any of the theoretical models investigated. However, the shape of the Budiansky equation, involving phase inversion at the intermediate composition, gave the best approximation. Similarly to the study on PUR/PEMA IPN compositions, a different modulus–composition pattern was observed at different temperatures. The storage modulus taken at 0°C seemed to have the phase inversion between the 70:30 and the 60:40 PUR/PS IPN compositions. From the moduli taken at 23°C, it appeared that phase inversion occurred at the 40:60 PUR/PS composition. However, the moduli taken at 100°C resulted in the phase inversion occurring at higher PS contents, namely, between the 30:70 and 20:80 compositions. Thus, it was confirmed that the temperature at which the moduli were taken had an important bearing on the shape of the modulus–composition plot. With the moduli taken at increasingly higher temperatures, the location where the logarithmic rule of mixing was crossed moved to higher PS contents. An intermediate temperature between the PUR and the PS transition might be most appropriate to conduct modulus–composition studies. A temperature of 67°C is roughly between 23°C (phase inversion at 40:60 PUR/PS) and 100°C (phase inversion at 20:80 PUR/PS). Consequently, phase inversion at 67°C might have taken place at the 30:70 PUR/PS IPN composition.

CONCLUSIONS

A gross phase morphology over the full PUR/PS IPN composition range was indicated by two separate loss factor peaks from DMTA. Both DMTA and MT-d.s.c. measurements revealed that the T_g of the PS transition increased with decreasing PS content in the IPN. The PS T_g increase (20°C by DMTA and 14°C by MT-d.s.c.) from the PS homonetwork to the 90:10 PUR/PS IPN was explained by an increase in interactions between the PUR hard segment and the π-electrons of the PS phenyl rings. The PUR T_g decreased at low PUR contents because of incomplete PUR network formation. The loss factor peak heights reflected the respective contents of PUR and PS and were of equal height at the 50:50 PUR/PS IPN composition. A particularly high increase in the PS loss factor height was observed

between the 30:70 (1.11) and the 20:80 (1.82) PUR/PS IPN compositions.

IPNs with good mechanical properties were prepared from the immiscible PUR/PS polymer pair. The stress at break increased with increasing PS content. A 10-fold increase occurred between the 30:70 (83 MPa) and 20:80 (830 MPa) PUR/PS IPN compositions. Both the strain at break (770%) and the toughness index (14 J) went through a maximum at the 70:30 PUR/PS IPN composition. Shore A and D hardness values increased with increasing PS contents. A particularly steep increase for Shore D was observed between the 30:70 (68) and the 20:80 (95) IPN compositions.

Modulus–composition studies revealed that the composition at which phase inversion apparently occurred depended on the temperature at which the storage moduli were taken. Taking E' at an intermediate temperature between the PUR and the PS T_g values resulted in phase inversion at the 30:70 PUR/PS IPN composition. This was in accordance with findings from the stress at break, Shore D measurements and with an earlier electron microscopy study. Thus, in the immiscible PUR/PS IPN composition series, phase inversion occurred at a higher high T_g component content (70% PS) than in semi-miscible PUR/PEMA IPNs (30% PEMA).

ACKNOWLEDGEMENTS

One of the authors (F.-U.S.) would like to acknowledge a grant from the German Academic Exchange Service, Deutscher Akademischer Austauschdienst DAAD.

REFERENCES

1. Hourston, D. J., Schäfer, F.-U., Gradwell, M. H .S. and Bates, J. S., *Polymer*, 1998, **39**(15), 3311–3320.
2. Kim, S. C., Klempner, D., Frisch, K. C., Frisch, H. L. and Ghiradella, H., *Polym. Eng. Sci.*, 1975, **15**, 339.
3. Lee, D. S. and Kim, S. C., *Macromolecules*, 1985, **18**, 2173.
4. Hourston, D. J. and Schäfer, F.-U., *Polymer*, 1996, **37**, 3521.
5. Hourston, D. J. and Schäfer, F.-U., *Polym. Adv. Technol.*, 1996, **7**, 273.
6. Reading, M., *Trends Polym. Sci.*, 1993, **8**, 248.
7. Song, M., Hammiche, A., Pollock, H. M., Hourston, D. J. and Reading, M., *Polymer*, 1995, **36**, 3313.
8. Paul, D. R. and Newman, S., *Polymer Blends*, Vols. 1 and 2. Academic Press, New York, 1978.
9. Nielson, L. E., *Mechanical Properties of Polymers and Composities*, Vols. 1 and 2, Marcel Dekker Inc., New York, 1974.
10. Kaplan, D. S., *J. Appl. Polym. Sci.*, 1976, **20**, 2615.
11. Yao, S., in *Advances in IPNs*, Vol. IV, eds. D. Klempner and K. C. Frisch, Technomic Publishing Company Inc., Lancaster, PA, 1994.
12. Schäfer, F.-U., Ph.D. Thesis, Loughborough University, Loughborough, UK, 1996.
13. Chughtai, N., Ph.D. Thesis, Lancaster University, Lancaster, UK, 1993.
14. Theocaris, P. S. and Kefalas, V., *J. Appl. Polym. Sci.*, 1991, **42**, 3059.
15. Cowie, J. M. G., in *Integration of Fundamental Polymer Science and Technology*, eds. L. A. Kleintjens and P. I. Lemstra, Elsevier Applied Science Publishers, London, 1986.
16. Kefalas, V., Theocaris, P.S. and Kontou, E., *Polym. Composites*, 1988, **9**, 229.
17. Garcia, D., *J. Polym. Sci. Polym. Phys. Ed.*, 1984, **22**, 1773.
18. Wang, F. C., Feve, M., Lam, T. M. and Pascault, J.-P., *J. Polym. Sci. Polym. Phys. Ed.*, 1994, **32**, 1315.
19. Tabka, M. T., Widmaier, J.-M. and Meyer, G. C., *Plast. Rubber Composites Proc. Appl.*, 1991, **16**, 11.
20. Mishra, V., Du Prez, F. and Sperling, L. H., *J. Polym. Mat. Sci. Eng.*, 1995, **72**, 124.
21. Billmeyer, F. W., *Textbook of Polymer Science*, 3rd edn, John Wiley & Sons, New York, 1984.
22. Sperling, L. H., *Interpentrating Polymer Networks and Related Materials*, Plenum Press, New York, 1981.
23. Technical literature, Operation instructions Zwick 3102, Ulm, 1975.
24. Davies, W. E. A., *J. Phys. D*, 1971, **4**, 1176.
25. Davies, W. E. A., *J. Phys. D*, 1971, **4**, 1325.
26. Budiansky, B., *J. Mech. Phys. Solids*, 1965, **13**, 223.
27. Kerner, E. H., *Proc. Phys. Soc.*, 1956, **B69**, 808.
28. Nielsen, L. E., *Predicting Properties of Mixtures*, Marcel Dekker, New York, 1978.
29. Nielsen, L. E., *J. Appl. Polym. Sci.*, 1977, **21**, 1579.
30. Dickie, R. A., in *Polymer Blends*, ed. D. R. Paul, Academic Press, New York, 1978.
31. Hourston, D. J. and Zia, Y., *J. Appl. Polym. Sci.*, 1983, **28**, 3745.
32. Ryan, A. J., Stanford, J. L. and Still, R. H., *Polymer*, 1991, **32**, 1426.
33. Kim, S. C., Klempner, D., Frisch, K. C., Radigan, W. and Frisch, H. L., *Macromolecules*, 1977, **10**, 1187.
34. Hourston, D. J. and Zia, Y., *J. Appl. Polym. Sci.*, 1983, **28**, 3849.
35. Allen, G., Bowden, M. J., Todd, S. M., Blundell, D. J., Jeff, G. M. and Davies, W. E. A., *Polymer*, 1974, **15**, 28.
36. Akay, M. and Rollins, S. N., *Polymer*, 1993, **34**, 1865.
37. Donatelli, A. A., Sperling, L. H. and Thomas, D. A., *Macromolecules*, 1976, **9**, 671.